

CUTTING FORCES AND CONSECUTIVE DEFORMATIONS AT MILLING PARTS WITH THIN WALLS

Ioan TĂNASE, Ionuț GHIONEA

Abstract: Some results of experimental researches and CAD-CAM simulations at milling plane surfaces of thin walls parts are presented in the paper. The cutting force measurement was done using a multi-component quartz dynamometer with a special data acquisition system for the cutting forces. The elastic deformation and the stress values in the machined part were determined by experimental tests and simulated using the FEM analysis. Depending on data that geometrically define the part and the cutting tool, their materials and the cutting parameters, are the values of the cutting force and power. There is presented a comparison of values obtained by measuring during the process with those established by applying FEM. This study results lead to some remarks and useful recommendations for determining the process parameters and the requirements for the technological system in the machining of parts having thin walls, with minimum deformations.

Key words: thin wall milling, cutting conditions, force measuring, deformation and stress analysis.

1. INTRODUCTION

Modern CAD-CAM techniques applied in the parts manufacturing processes have a large use in all the mechanical industry domains. In the literature [2] are presented many results of FEM applications in order to determine the elastic deformations values and the stresses induced in parts at the contact with the tools during the machining processes. The influences of the technological system (machine-tool, tools, fixture devices) determine dimensional variations and irregularities of the processed surfaces, [5] dynamical behavior of the machine-tool in the cutting process and also the premature wear of the cutting edges [7].

The results of the surfaces generation by simulation, with the aid of CAM techniques offer a large number of data: machining times, surface accuracy, behavior of the machine-tool in working conditions (cutting forces and power consumption).

Also, by FEM simulations there are determined the stress and deformation values created by the cutting forces in the thin walls of the analyzed parts [1, 5]. For the optimization of the technological process there are considered and applied various criteria, software environments, tables of data.

2. THE CAM SIMULATION

Preparing the part for processing on a machine-tool with numerical control involves the generation of command information, all data is then stored in a preset order within a storage device.

Programs can be generated directly on the machine, the operator writes the necessary instructions using the interface or by using a CAD-CAM program and a virtual model of the piece [3]. Defining the piece in a CAD environment is used as the entry data to generate the program with one of the complex existing programming

languages. Thus, the simulation is justified to optimize the process because CAM programs elaborate the NC machine code. For the study, it is considered a part having its 3D model made in CATIA Part Design module and presented in Fig. 1.

The overall dimensions of the stock part are 80×80×37 mm. This part has a side thin wall and a cavity. The machined surface of this thin wall is marked with S1 and the wall has 1 mm thickness. The stock part has two side pockets for direct clamping on the machine-tool table. The CAM simulation involves multiple passes in conditions of roughing and finishing millings with specific technological parameters.

The machining process of the part was simulated using a 3-axis CNC vertical milling machine tool with the following main characteristics:

- spindle speed: 18000 rpm with infinite variable speed range (direct drive spindle),
- the power of the main spindle motor: $P = 15$ kW (continuous rating),
- working strokes on axes $X = 550$ mm, $Y = 450$ mm, $Z = 500$ mm,
- machining feed rate max: 8000 mm/min and rapid feed rate: 20000 mm/min;
- the machine tool has a CNC Sinumerik controller.

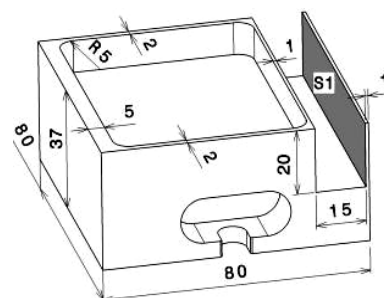


Fig. 1. 3D model of the analyzed part.

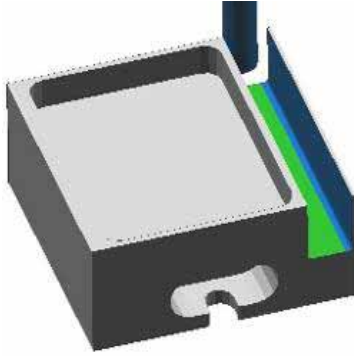


Fig. 2. Finish milling of S1 surface.

The tools used in manufacturing simulation are chosen from a company catalogue [9]. Also, the tool holders are in correspondence with the spindle nose and the holding system of the machine-tool. Only two steps of the CAM simulation (surface S1) in the case of a steel (OLC45) work piece, 190 HB are presented below (figure and parameters):

a. *Slot mill*, three passes, $D_c = 12$ mm - tool diameter, $h_m = 0.06$ mm – average chip thickness, $v_c = 280$ m/min - cutting speed, $n_c = 7400$ rpm - spindle speed, $v_f = 2900$ mm/min - feed speed, $P_c = 13$ kW - cutting power for removal of chips, $M_c = 17$ Nm - cutting torque, $Q = 235$ cm³/min - metal removal rate, $f_z = 0.1$ mm – feed per cutting edge, $a_p = 6.6$ mm - cutting depth, $z_c = 4$ – number of teeth, $t_m = 6$ s – machining time, $t_t = 9$ s – total time.

b. *Side wall finishing end mill* (Fig. 2), two passes, $D_c = 10$ mm, $h_m = 0.01$ mm, $v_c = 300$ m/min, $n_c = 9500$ rpm, $v_f = 1900$ mm/min, $P_c = 1.7$ kW, $M_c = 1.7$ Nm, $Q = 19$ cm³/min, $f_z = 0.05$ mm, $a_p = 20$ mm, $a_e = 0.5$ mm – working engagement, $z_c = 4$.

Figure 3 presents a fragment of the NC code obtained after the CAM simulation [3] in the case of the finishing milling.

```
N260 ;=== TOOL CHANGE ===
N290 T2 M06
N300 D2
N310 G0 G90 G40 G17
N320 G94 F2900 S7400 M3
N330 G64 SOFT
N340 G1 X33.45 Y30 Z-34 S9500 F4000
N350 Z-57
N360 Y40 F1900
N370 Y120
N380 Y130
N390 G0 Z-36
N400 G0 X33.95 Y30
N410 G0 Z-57
N420 G1 Y40 F0.1
N430 Y120
N440 Y130
N450 Z-34 F4000
N460 M5
N470 M5 M9
N480 M30
```

Fig. 3. Fragment of the NC code.

3. DEFORMATION AND STRESS ANALYSIS BY FEM SIMULATION

In this FEM simulation it is considered a finishing end mill with the diameter $D_c = 10$ mm, number of cutting edges $z_c = 4$, pitch of the helical cutting tooth $L_{sh} = 28$ mm, helix angle $\omega = 50^\circ$ [6].

On the contact line between the milling edge and the part there are created three cutting spots placed on the height of the helical pitch, shown in Fig. 4.

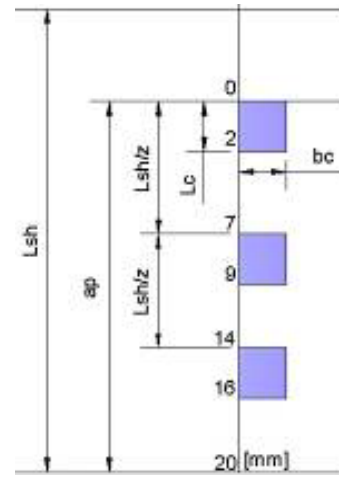


Fig. 4. The dimensions and positions of the cutting spots.

In order to establish these spots where the radial medium cutting force is applied it was necessary to determine the contact length of each helical edge with the part. The dimensions and the positions of the spots depend on the contact angle φ between the part and the cutting edge and the helical pitch of the cutting teeth, determined using the equations (1), (2) and (3).

$$\varphi = 2 \cdot \sqrt{\frac{a_e}{D_c}} = 0.447 \text{ [rad]}, \quad (1)$$

$$L_c = \frac{L_{sh} \cdot \varphi}{2\pi} = \frac{28}{\pi} \sqrt{\frac{0.5}{10}} = 2 \text{ [mm]}, \quad (2)$$

$$b_c = \sqrt{0.25 \cdot D_c^2 - (0.5 \cdot D_c - a_e)^2} = 2.18 \text{ [mm]}, \quad (3)$$

where: L_c – length of the cutting spot, b_c – width of the cutting spot and L_{sh} - helical pitch of the cutting edge, $a_e = 0.5$ mm – working engagement.

The medium cutting force acting on the contact spots is determined using the values for cutting power P_c depending on the cutting parameters [4]:

$$F_{tm} = \frac{60000 \cdot P_c}{v_c} \text{ [N]}, \quad (4)$$

and it has the values: 287 N (roughing), respectively, 203 N (finishing).

The radial medium cutting force (which is practically applied on the three spots) is $F_{rm} = (0.5 \dots 1) \cdot F_{tm}$, considered $F_{rm} = 0.9 \cdot F_{tm} = 183$ N.

As follows, there are presented some results of FEM simulations and analysis in the cases of the part being machined of steel OLC45. Thus, the radial medium cutting force is $F_{rm1} = 61$ N on each of the three cutting spots.

Figure 5 presents the deformations of the thin wall in the case that the cutting force is applied in the middle area. The simulation results show that the maximum deformation of machined wall in the middle area is 0.108 mm, very great value, compared to 1 mm the machined wall thickness.

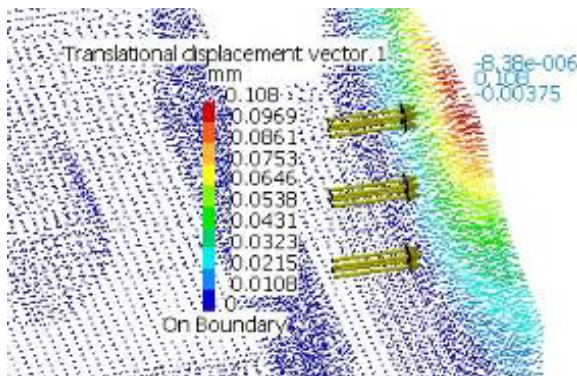


Fig. 5. Deformations of the thin wall in the middle area.

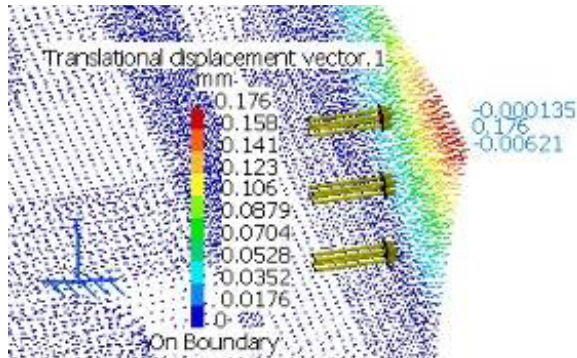


Fig. 6. Deformations of the thin wall at one of the ends.

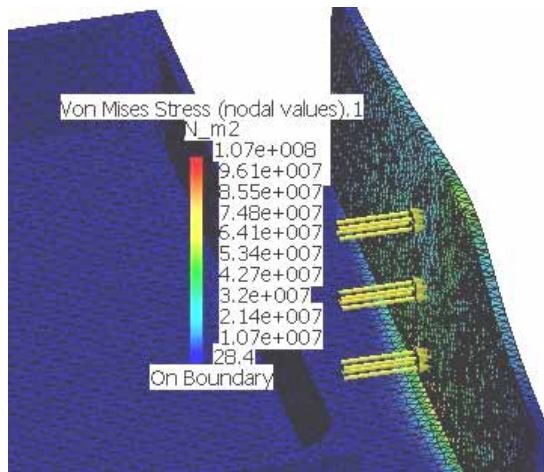


Fig. 7. Von Mises stresses of the thin wall in the middle area.

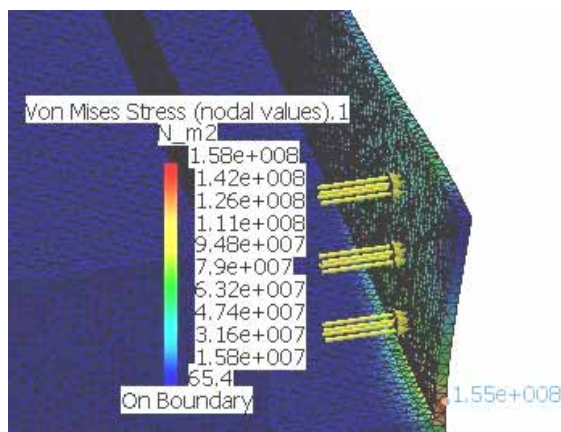


Fig. 8. Von Mises stresses of the thin wall at one of the ends.

Also, Fig. 6 shows the deformations when the cutting force is applied on one of the thin wall's ends. The maximum deformation at the free end of machined wall is 0.176 mm, an inadmissible value, due to significant variation of the wall thickness which results.

Using the CATIA software FEM analysis capabilities, there is simulated the distribution of the stresses in both situations.

Figure 7 shows the Von Mises Stresses calculated in the case of the force applied in the middle area of the thin wall. For a force of 61 N (on each cutting spot) the results are: maximum stress = 1.07×10^8 N/m² and max. elastic deformation $\Delta x = 0.108$ mm (Fig. 5) with an error of 27.7 %.

Figure 8 shows the Von Mises Stresses calculated in the case the force applied in one of the ends of the thin wall. For a force of 61 N (on each cutting spot) the results are: maximum stress = 1.58×10^8 N/m² and maximum elastic deformation $\Delta x = 0.176$ mm (Fig. 6) with an error of 31.2 %.

The considered steel has the yield strength of 2.5×10^8 N/m².

In the FEM practice, an error of 20% – 35% is acceptable and it is considered close to the real case [2]. Anyway, in both situations for the flat surface S_1 , the maximum stresses are lower than the materials' yield strengths, so the thin wall is deformed only in the elastic domain.

4. EXPERIMENTAL RESEARCHES

4.1. Experimental setup

The purpose of the experimental researches was to determine the elastic deformations of the thin wall for the considered part, in real conditions of milling. In the process it was used an universal milling machine, type FN-32. Also, for the cutting tool it was chosen a solid carbide end mill CoroMill Plura (GC 1620), with diameter $D_c = 10$ mm, tool helix angle = 50° , helical pitch of the cutting teeth = 28 mm, total length = 100 mm, length of the active part = 26.5 mm.

The cutting conditions were: cutting speed $v_c = 63$ m/min, feed per tooth $f_z = 0.02 \dots 0.04$ mm, cutting depth $a_p = 20$ mm, working engagement $a_e = 0.2 \dots 0.5$ mm. The milling process was done without cooling, down-milling method.

It is recommended to avoid up-milling procedure, because of strong chatter or high frequency vibrations occurring, related to low feed per tooth.

The experimental arrangement for the determination of cutting forces and for the measurements of elastic deformations was composed of the next main components (Fig. 9 and Fig. 10): work piece (1), Quartz 3 component Dynamometer Type 9257 B Kistler (2) fixed on the machine table (5); Multi-Channel Charge Amplifier for Multicomponent – Force Measurement Type 5070 A (6); Data acquisition board Type PCIM-DAS1602/16 (7); DynoWare Type 2825A data acquisitions and manipulation software [8]; PC with Windows XP. The milling cutter (3) was fixed in the main spindle of the tilting milling head (4), through a tool holder.

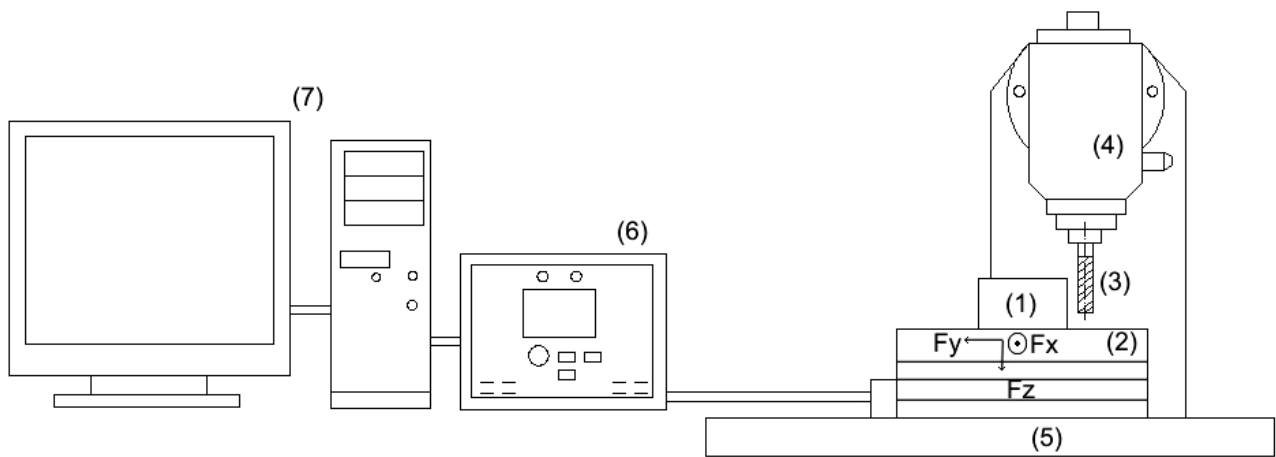


Fig. 9. View of experimental setup

The components of the cutting force, F_x , F_y and F_z were measured with the dynamometer on the directions of the considered reference system (Fig. 9). The component F_x is normal oriented on the surface of the processed wall and cause its deformation. The component F_y is oriented on the direction of feed movement, and the F_z component is on the direction of tool's axis. The measuring of the elastic deformation of the machined thin wall $S1$ (Fig. 11) was done with a dial gauge C with a division of 0.001 mm whose detector was located at the middle of the wall length of the work piece W , at its maximum height.

The tool T is presented at the end of the finishing milling pass, done by down milling. In the cutting zone there are chips Ch resulted from machining process.



Fig. 10. Experimental setup.



Fig. 11. Machining area.

4.2. Results of the experimental determinations

The cutting forces were measured in conditions of roughing and finishing milling, with corresponding cutting speeds. 12 measurements were done in order to determine the cutting forces and the maximum deformations of the thin wall, machined from the thickness of 3.5 mm to 1 mm. Within each measurement it was accomplished a file with processed data and the measurements results of 8 components using the Kistler dynamometer signals. Every data file contains a page with comments (Fig. 12) which allows the user to annotate the conditions for each measurement.

By processing the acquired data files with DynoWare type 2825 A, there are obtained variations diagrams of the cutting forces components previously selected by the user, and also the minimum, medium and maximum values on the chosen intervals of time, as needed (e. g. for a tool rotation).

The numerical values of each force component may be determined for each moment or interval of the determination using options from the program toolbar.

Some results for a few of the 12 experimental determinations are shown in Table 1. The values of the measured forces are determined directly by the cutting depth a_e and by the feed per cutting edge f_z , all the other parameters being maintained constant.

Comments		File, Date, Time	
Document title:			
Cutter D10-9			
Remarks:			
CoroMill-Plura D 10 mm, z=4			
Down milling			
Material:			
DLC45			
Tool:			
Dc = 10 mm, z = 4 teeth			
$V_c = 63$	m/min	$f = 0.16$	mm/rev
$\alpha_p = 20$	mm	$n = 2000$	rpm
$v_f = 315$	mm/min	$a_e = 0.5$	mm
<input checked="" type="checkbox"/> Cutting Force <input type="checkbox"/> Documentation Mode			
<input checked="" type="checkbox"/> Show Documentation Between Acquisition Cycles			

Fig. 12. Comments for the cutting conditions.

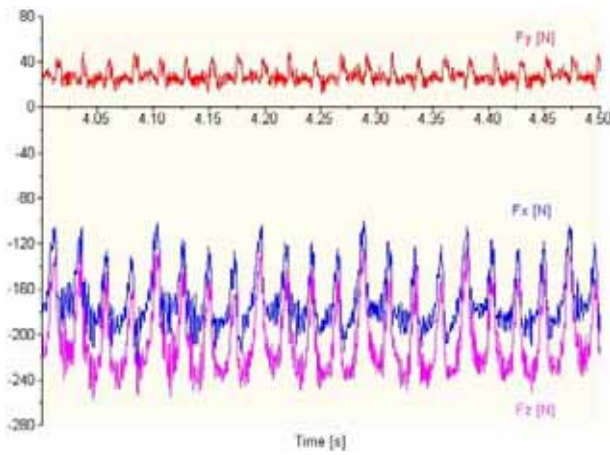


Fig. 13. Cutting forces for the determination D10-1.

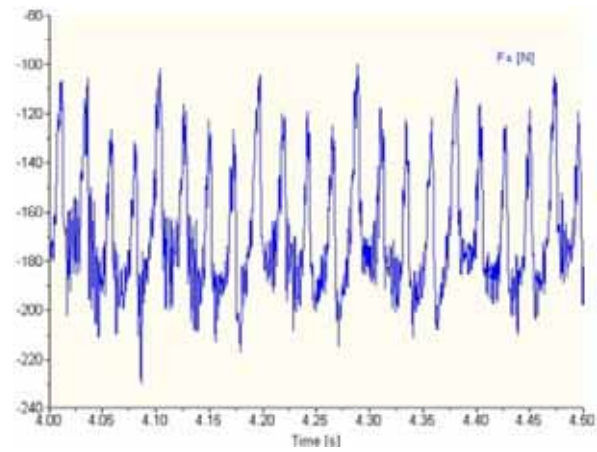


Fig. 14. Detail of cutting forces F_x for the determination D10-1.

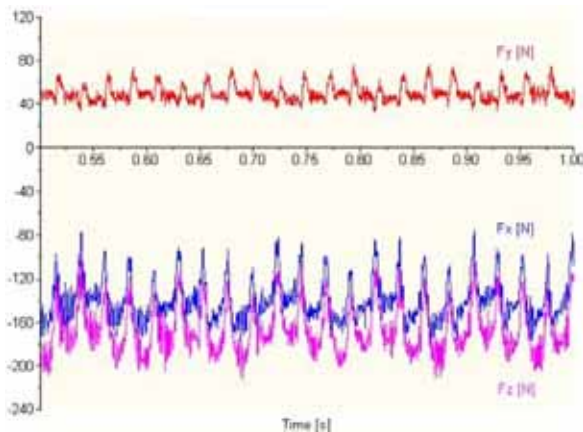


Fig. 15. Cutting forces for the determination D10-6.

The components F_x , F_y and F_z are determined at the first tool's pass, noted with D10-1, on a time interval of 0.5 s and they are presented in the Figure 13. The graphics appear overlapped and they could be distinguished by different colors.

In the studied case it presents a great interest the F_x force component (Fig. 14) oriented normal to the surface of the machined thin wall.

During the milling pass for a wall thickness of 2 mm, test noted with D10-6, there were obtained the components of the cutting force represented in Fig. 15. The cutting conditions in this test were the same as for the test D10-1 and the measured values of force components are closely related. Also, the general aspects of cutting forces variations presented in Figs. 13 and 15 are quite similar.

For another test D10-9, the cutting force components have the variations represented in the Fig. 16, for a wall thickness of 1.5 mm.

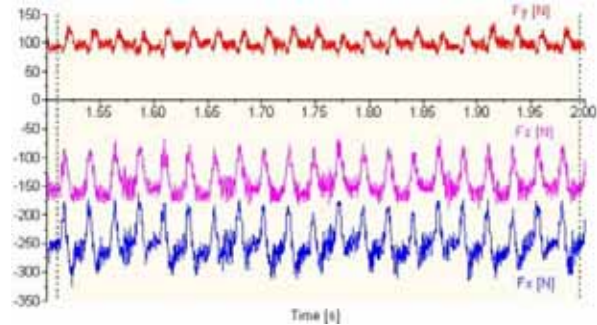


Fig. 16. Cutting forces for the determination D10-9.

The feed per tooth was greater (see Table 1) and the cutting force components present a sensible increase, compared to D10-6 test.

The general aspect of forces diagrams is modified: F_x component reaches greatest absolute value and as a consequence the deflection of the machined wall Δx has increased.

The last milling pass, test D10-12 (see Table 1) was accomplished with the same cutting conditions as for the test D10-9.

The cutting force components measured values present a little decrease, compared to D10-9 test. This is due to elastic deformation of machined thin wall and, as a consequence the decrease of actual working engagement a_e compared to settled value.

Also, for the determination of the cutting force component F_x , it was applied a calculus algorithm using some data from the Coromant catalogue, or a specialized software CoroGuide for the process parameters.

For the rough milling regime, corresponding to the test D10-9, the average tangential force, using CoroGuide data results: $F_{med9} = 287$ N.

Table 1

Experimental results at forces measurements

Det. No.	F_x [N]		F_y [N]		F_z [N]		f_z [mm/tooth]	a_e [mm]	Thickness wall [mm]	Deformation Δx [mm]
	med	max	med	max	med	max				
D10-1	-170	-216	26	52	-205	-263	0.025	0.5	3	0.008
D10-6	-149	-184	55	81	-167	-215	0.025	0.5	2	0.012
D10-9	-248	-325	100	134	-141	-187	0.04	0.5	1.5	0.035
D10-12	-227	-305	98	122	-135	-174	0.04	0.5	1	0.14

The average radial force is: $F_{rmed9} = (0.5...1) F_{med9} = 229$ N. The measured value for F_x component in the D10-9 determination was $F_{xmed} = 248$ N and the corresponding deformation was $\Delta x = 0.035$ mm.

For the finish milling regime, corresponding to the test D10-6, the calculated values for these two force components are: $F_{rmed6} = 203$ N and $F_{med6} = 162$ N. The measured value for F_x component in the D10-6 determination was $F_{xmed} = 149$ N, for the calculated radial force F_{rmed6} .

Making a comparison between the results obtained by measurement of the component F_x with a dynamometer and the calculated values of the average radial force is found that the differences are below 10%, thus proving out the validity of calculations and measurements made in the experimental tests.

The diagrams of F_x , F_y and F_z components of the cutting force shows relatively large cyclical variations with the corresponding period of time of a tool rotation.

Thus, in the actual working conditions, when the spindle speed is $n_c = 2000$ rpm, the corresponding time to a tool rotation is 0.03 s. This force variation is due to inherent radial run-out of the edge related to the tool rotation axis, and also to a low feed per tooth.

5. CONCLUSIONS

The determination of the cutting forces that the cutting edges react on the machined surface was made using an experimental arrangement based on multi-component Quartz dynamometer.

The value of the thin wall's maximum elastic deformation, measured during the finish milling is very high compared with the wall thickness. Thus the machined wall thickness results uneven.

This shows that the cutting regime (the parameters a_e and f_z) has to be decreased if the permissible deviations (precision required during real machining by milling) are smaller than the resulted maximum elastic deformation.

The elastic deformations Δx are higher at both ends of the wall (0.176 mm) compared to the deformation at the middle of the wall (0.108 mm). The result is an unexpected great variation of the wall thickness in both directions, length and height. The measured values of the radial forces and elastic deformation Δx are in a good correspondence with the calculated values.

Also, these deformations corresponding to the considered working regime seem to be unacceptable influencing the accuracy of the machined surfaces. If the aim is a higher precision, the parameters of the machining regime should be decreased and the simulation process resumed.

REFERENCES

- [1] Budak, E., Altintas, Y. (1994). *Peripheral milling conditions for improved dimensional accuracy*, International Journal of Machine Tools and Manufacture. 34 (7), ISSN 0890-6955, pp. 907-918.
- [2] Constantinescu, N. I., Sorohan, Șt., Pastramă, Șt. (2006). *The practice of finite element modeling and analysis*, Edit. Printech, Bucharest, ISBN 978-973-718-511-2.
- [3] Ghionea, I. (2009). *CATIA v5. Aplicații în ingineria mecanică* (CATIA v5. Applications in mechanical engineering). Edit. Bren, ISBN 978-973-648-843-6, Bucharest.
- [4] Ghionea, I., Ghionea, A., Tănase, I. (2009). *Application of CAM-FEM techniques in the establishment of milling conditions of the parts with thin walls surfaces*, 4th International Conference Optimization of the Robots and Manipulators, OPTIROB, 28-31 May, pp. 27-32, Edit. Bren, Bucharest, ISSN 2066-3854.
- [5] Rao, S. V., Rao, M. V. P. (2006). *Tool deflection compensation in peripheral milling of curved geometries*, International Journal of Machine Tools and Manufacture. Design, Research and Application 46 pp. 2036-2043.
- [6] Tănase, I. (2009), *Scule așchietoare* (Cutting Tools), Edit. BREN, ISBN 978-973-648-849-8, Bucharest.
- [7] Trent, E., Wright, P. (2000). *Metal cutting*, Butterworth Heinemann, Oxford, Boston.
- [8] *** (2008). *Operating Instructions KISTLER Instrumente* AG, Switzerland.
- [9] *** (2008). *Metalworking products CoroGuide 08.2*, SANDVIK Coromant.
- [10] *** (2005). *Metalcutting Technical guide*, SANDVIK Coromant, C-2900:3 ENG/01, Printed in Sweden by Elanders.

Authors:

PhD, Eng, Ioan TĂNASE, Professor, University "Politehnica" of Bucharest, Machine and Production Systems Department, Bucharest, Romania.

E-mail: tanase.ioan@yahoo.com

Eng, Ionuț GHIONEA, Lecturer, University "Politehnica" of Bucharest, Department of Machine Manufacturing Technology, Bucharest, Romania.

E-mail: ionut76@hotmail.com